Supporting Information

Switchable glycan probe enables pH-dependent modulation of UDP-glucose: glycoprotein glucosyltransferase through a responsive aglycone

Mitsuaki Hirose,*[1] Yuka Suzuki,[1] Rentaro Miyuki,[1] Kosuke Oki,[1] Keirin Sato,[1] Akihiro Yokoyama,[1] and Kiichiro Totani *[1]

[1] Graduate School of Science and Technology, Seikei University, 3-3-1 Kichijoji-kitamachi, Musashino-shi, Tokyo 180-8633, Japan

*Corresponding authors

Mitsuaki Hirose; mitsuaki-hirose@st.seikei.ac.jp

Kiichiro Totani; ktotani@st.seikei.ac.jp

Contents

Reagents and others

All reagents were purchased from the Wako Pure Chemical Industries (Osaka, Japan), Kanto Chemicals Co. Inc. (Tokyo, Japan), Tokyo Chemical Industries Co. Ltd. (Tokyo, Japan), or Nacalai Tesque (Kyoto, Japan). **G1M9-Asn-Fmoc** was obtained from KH-i Lab KH Neochem. Co. Ltd (Kanagawa, Japan). TLC was performed on precoated glass plates using silica gel (Merck, 60, F254) and detected by ultraviolet light (254 nm) and/or by staining reagents such as Orcinol/H_2SO_4 and $(NH_4)_2MoO_4$/$Ce(SO_4)_2$/H_2SO_4.

M9-Asn-Fmoc was prepared from egg yolk according to the previously reported procedures with minor modifications [S1].

UGGT1 was prepared from Wistar rat liver (10-week, male), which was purchased from Japan SLC, Inc. (Shizuoka, Japan), according to the previous procedure [S2].

Nuclear magnetic resonance (NMR) spectroscopy

1D ^{1}H NMR spectra were recorded on a JEOL JNM-ECA-500 (500 MHz) spectrometer; DHO (δ_H = 4.79 ppm) was used as an internal reference.

High-resolution mass spectrometry (HRMS)

HRMS were recorded on a Thermo Fisher Scientific (MA, USA) Q Exactive hybrid quadrupole-Orbitrap mass spectrometer equipped with an electrospray ionization (ESI) source, operated in the positive- or negative-ion mode using MeOH as the solvent.

High performance liquid chromatography (HPLC)

HPLC was performed using a JASCO Corporation liquid chromatography system: a DG-2080-53 system controller, an UV-2077 Plus (273 nm), PU-2089 Plus pump, an AS-2051 Plus autosampler, and a CO-2065 Plus column oven at 40 ºC.

Ultra performance liquid chromatography (UPLC)

UPLC was performed using a Waters liquid chromatography system at an Acquity I class: an empower3 system controller, an FLR detector (For **M9-Asn-Fmoc**: λ_{em} = 273 nm, λ_{ex} = 311 nm; For **M9-Asn-FL**: λ_{em} = 494 nm, λ_{ex} = 521 nm), a Binary solvent manager pump, a Sample manager-FTN autosampler, and a CH-A column oven at 40 ºC.

Ultraviolet-visible (UV-vis) measurement

UV–vis absorption spectra were measured with V-650 spectrophotometer from JASCO (Tokyo, Japan).

Quantum chemical calculation of $GlcNAc_2$-Asn-FL

The mono- and di-anion models (**$GlcNAc_2$-Asn-FL**) of fluorescein derivative containing $GlcNAc_2$ disaccharide instead of **M9-Asn-FL** were used for the computational study for simplicity. The initial structures were constructed on a Windows 11 PC with the GaussView 6 (Gaussian, Inc., Pittsburgh, PA). The structures were fully optimized by the density functional theory (DFT) calculations using the B3LYP [S3] functional with the 6-31G+(d) basis set [S4] in Gaussian 16 software (Gaussian, Inc., Pittsburgh, PA) [S5]. Vibrational frequency calculations were then performed at the same level of theory to confirm that the optimized structures correspond to minima (no imaginary frequencies). The geometry-optimized structures were used for docking simulations.

Docking simulations of $GlcNAc_2$-Asn-FL ligands with human UGGT1

The AlphaFold-predicted structure [S6] of human UGGT1 (UniProt ID: Q9NYU2) was used as the receptor model. A simplified glycan probe model, **$GlcNAc_2$-Asn-FL**, was used as the ligand, and both the monoanionic and dianionic forms of the fluorescein moiety were examined. Docking simulations were performed using AutoDock Vina v1.1.2 [S7]. Because the precise aglycone-recognition site of UGGT1 remains unknown, the docking search space was focused on hydrophobic surface regions surrounding the TRXL2 and TRXL3 domains, which have been proposed to contribute to substrate recognition. The grid box was centered at x = −13.0, y = 15.1, and z = 21.7 Å, with dimensions of 50 × 50 × 50 Å. The exhaustiveness, number of output binding modes, and energy range were set to 32, 20, and 5 kcal mol^{-1}, respectively. For each ligand, the top-ranked docking pose with the lowest predicted binding energy was selected for further analysis and visualization as Fig. S7. The predicted docking models were visualized using PyMOL.

*Synthesis of **M9-Asn***

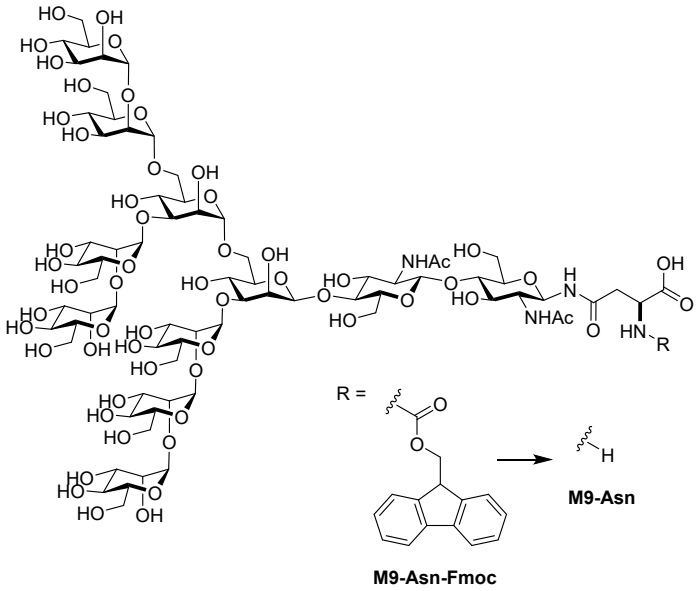

To a stirred DMF (350 μL) solution of **M9-Asn-Fmoc** (3.6 mg, 1.6 μmol) was added piperidine (40 μL) and ddH_2O (10 μL) at 0 ºC, and then the mixture was stirred at room temperature for 30 min under air. The reaction progress was monitored by TLC (H_2O/2-propanol = 2/3, *v*/*v*, R_f = 0.33). After evaporation of the solvents, the reaction mixture was diluted with ddH_2O, washed with EtOAc three times. After evaporation of the solvents, the residue was purified by Sep-Pak (2g) (ddH_2O = 100) to give a **M9-Asn** quantitatively as a white solid: ^{1}H NMR (500 MHz, D_2O) δ/ppm = 5.40 (1H, s, H-1 of Man), 5.33 (1H, s, H-1 of Man), 5.30 (1H, s, H-1 of Man), 5.14 (1H, s, H-1 of Man), 5.06 (1H, d, *J* = 9.7 Hz, H-1 of GlcNAc), 5.05–5.03 (3H, m, H-1 of Man × 3), 4.86 (1H, s, H-1 of Man), 4.76 (1H, H-1 of Man), 4.60 (1H, d, *J* = 8.0 Hz, H-1 of GlcNAc), 4.22–3.52 (67H, m, H-2, -3, -4, -5, -6, and -6’ of Man × 9, GlcNAc × 2, α-CH of Asn), 2.92 (1H, dd, *J* = 4.6, 17.2 Hz, β-CH of Asn), 2.85 (1H, dd, *J* = 6.9, 17.2 Hz, β-CH of Asn), 2.06, 2.00 (each 3H, s, Ac of GlcNAc), [NH_2 and COOH peaks were not observed.].

*Synthesis of **M9-Asn-FL***

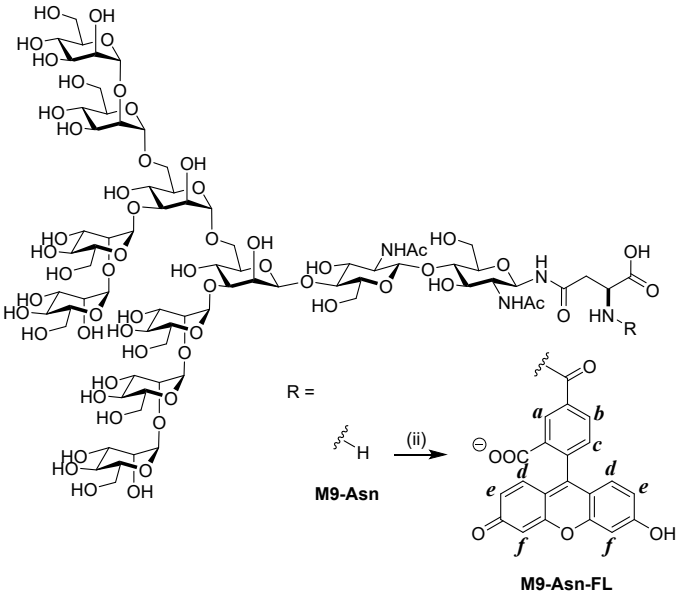

To the stirred DMF solution of **M9-Asn** (3.2 mg, 1.6 μmol) was added FL-OSu (3.0 mg, 6.4 mmol) at 0 °C, and then the mixture was stirred 37 °C for 2 h under air in the dark. The reaction mixture was warmed to 45 °C and stirred for 1 h. The reaction progress was monitored by TLC (H_2O/2-propanol = 2/3, R_f = 0.66). After the reaction mixture was evaporated *in vacuo*, the residue was purified by cotton HILIC (MeCN/H_2O = 90/10 → 80/20 → 70/30 → 60/40 → 50/50 → 0/100, *v*/*v*) and HPLC (Insert Sustain AQ-C18, 5 μm, 10 mm ϕ × 250 mm, 40 ℃, liner gradient CH_3OH/H_2O = 0/100 → 50/50 over 75 min, 3.0 mL/min, detection wavelength 521 nm) to give a **M9-Asn-FL** (2.5 mg, 1.1 μmol, 69%) as a pale-yellow solid: ^{1}H NMR (500 MHz, D_2O) δ/ppm = 8.21 (1H, s, H_a of fluorescein), 8.00 (1H, d, *J* = 8.0 Hz, H_b of fluorescein), 7.47 (1H, d, *J* = 8.0 Hz, H_c of fluorescein), 7.19 (2H, t, *J* = 8.0 Hz, H_d × 2 of fluorescein), 6.70–6.64 (4H, m, H_e × 2 and H_f × 2 of fluorescein), 5.39 (1H, s, H-1 of Man), 5.32 (1H, s, H-1 of Man), 5.29 (1H, s, H-1 of Man), 5.13 (1H, s, H-1 of Man), 5.08 (1H, d, *J* = 9.2 Hz, H-1 of GlcNAc), 5.05–5.02 (3H, m, H-1 of Man × 3), 4.85 (1H, s, H-1 of Man), 4.72 (1H, s, H-1 of Man), 4.58 (1H, d, *J* = 9.2 Hz, H-1 of GlcNAc), 4.22–3.22 (67H, m, H-2, -3, -4, -5, -6, and -6’ of Man × 9, GlcNAc × 2, α-CH of Asn), 3.00 (1H, dd, *J* = 3.4, 16.0 Hz, β-CH of Asn), 2.84 (1H, dd, *J* = 9.2, 16.0 Hz, β-CH of Asn), 2.02, 1.81 (each 3H, s, Ac of GlcNAc); HRMS (ESI) found: *m/z* = 2378.7224, calcd for $[^{12}C_{94}{}^{13}C_1H_{134}N_4O_{64} + Na]^+$, 2378.7280.

*Synthesis of **G1M9-Asn-FL***

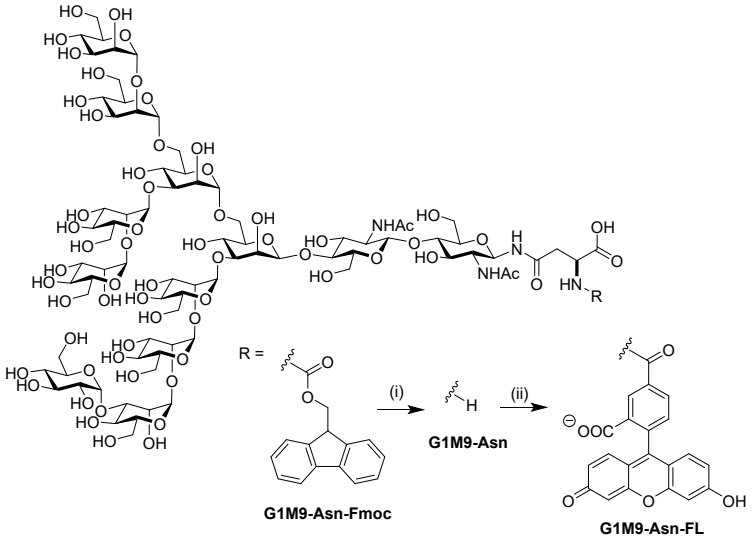

To a stirred DMF solution (800 μL) of **G1M9-Asn-Fmoc** (0.81 mg, 0.34 μmol) was added piperidine (200 μL) at 0 ºC, and then the mixture was stirred at room temperature for 1 h under air. The reaction progress was monitored by TLC (H_2O/2-propanol = 2/3, *v*/*v*, R_f = 0.12). After evaporation of the solvents, the reaction mixture was diluted with ddH_2O, washed with EtOAc three times. After evaporation of the solvents, the residue was purified by Sep-Pak (2g) (ddH_2O/MeOH = 10/0 → 5/5 → 0/10) and Sephadex G-10 (ddH_2O = 100) to give a **G1M9-Asn**, which was used in next step without calculation of the yield: HRMS (ESI) found: *m/z* = 2182.7350, calcd for $[^{12}C_{79}{}^{13}C_1H_{134}N_4O_{63} + Na]^+$, 2182.7331.

To a stirred DMF solution (100 μL) of the above **G1M9-Asn** was added a mixture of FL-OSu (0.40 mg, 0.76 μmol) and DIPEA (220 μL, 1.26 mmol). Additional portions of FL-OSu (0.47 mg, 0.89 μmol and 0.43 mg, 0.82 μmol) were added at 15 min interval. The resulting solution was stirred at 45 °C for 19 h under Ar. The reaction progress was monitored by TLC (H_2O/2-propanol = 2/3, *v*/*v*, R_f = 0.59). After evaporation of the solvents, the residue was purified by cotton HILIC (ddH_2O/CH_3CN = 1/9 → 1/4 → 3/7 → 2/3 → 1/1 → 0/10) and HPLC (Insert Sustain AQ-C18, 5 μm, 10 mm ϕ × 250 mm, 40 ºC, liner gradient CH_3CN/H_2O = 0/100 → 50/50 over 70 min, 3.0 mL/min, detection wavelength 521 nm) to give **G1M9-Asn-FL** (0.47 mg, 0.19 μmol, 56% for the 2 steps) as a pale-yellow solid: HRMS (ESI) found: *m/z* = 2516.7820, calcd for $[^{12}C_{100}{}^{13}C_1H_{144}N_4O_{69} - H]^-$, 2516.7842.

UGGT1 enzymatic assay

To an aqueous 10 mM MES (pH 5.5, 6.0 and 6.5), HEPES (pH 7.0 and 7.5), or Bicine buffer solution (pH 8.0, 8.5 and 9.0) containing 0.6% (*v*/*v*) Triton X-100, 10 mM $CaCl_2$, 1 mM dMJ, and 1 mM dNJ, was added UGGT1 enzyme (0.5 mg protein/mL) [S3], and then the mixture was incubated for 30 min at 37 °C under air in the dark. **M9-Asn-Fmoc** (100 μM) or **M9-Asn-FL** (100 μM) as substrate and 1 mM UDP-Glc were added to the mixture solution, which was incubated at 37 °C. To stop the enzymatic reaction, a portion of the mixture was added CH_3CN and ddH_2O. The resulting precipitates of proteins were removed by centrifugation (20,000 × *g*, 20 min, 4 °C). The supernatant was collected to obtain samples for HPLC analysis. HPLC condition: Waters ACQUITY UPLC Glycan BEH Amide column (1.7 mm, 2.1 ϕ mm × 150 mm), CH_3CN/50 mM HCO_2NH_4 (pH 4.5), linear gradient from 65/35 to 52/48 over 10 min, 0.37 mL/min, column oven was set to 40 °C, λ_{ex} = 263 nm, λ_{em} = 317 nm for **M9-Asn-Fmoc**, λ_{ex} = 494 nm, λ_{em} = 521 nm for **M9-Asn-FL**.

UGGT1 enzymatic assay under pH-shift condition

To an aqueous 10 mM MES (pH 6.0) or Bicine buffer solution (pH 8.5) containing 0.6% (*v*/*v*) Triton X-100, 10 mM $CaCl_2$, 1 mM dMJ, and 1 mM dNJ, was added UGGT1 enzyme (0.5 mg protein/mL) [S3], and then the mixture was incubated for 30 min at 37 °C under air in the dark. **M9-Asn-FL** (100 μM) as substrate and 1 mM UDP-Glc were added to the mixture solution, which was incubated at 37 °C for 5 h. After the mixture was added to 1 M MES (1 μL, pH 6.0) or Bicine buffer solution (1 μL, pH 8.5), the resulting solution was incubation for additional 19 h. To stop the enzymatic reaction, a portion of the mixture was added CH_3CN and H_2O. The resulting precipitates of proteins were removed by centrifugation (20,000 × *g*, 20 min, 4 °C). The supernatant was collected to obtain samples for UPLC analysis. UPLC condition was same as above mentioned in section UGGT1 enzymatic assay.

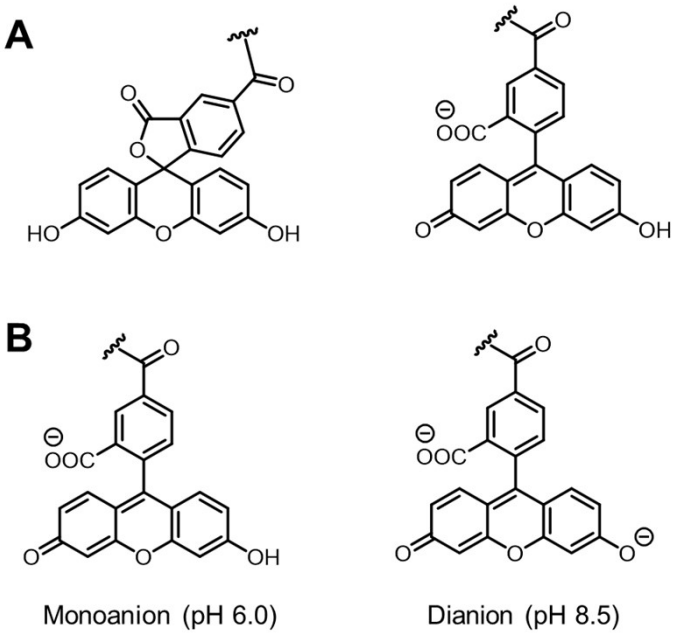

Fig. S1. (A) Chemical structures of closed-lactone (left) and open-quinoid forms (right) in fluorescein derivatives. (B) pH-dependent structural changes of the fluorescein moiety in **M9-Asn-FL**. The fluorescein moiety exists predominantly in the monoanionic form (with minor neutral/lactone species) at pH 6.0 and as the dianionic form at pH 8.5.

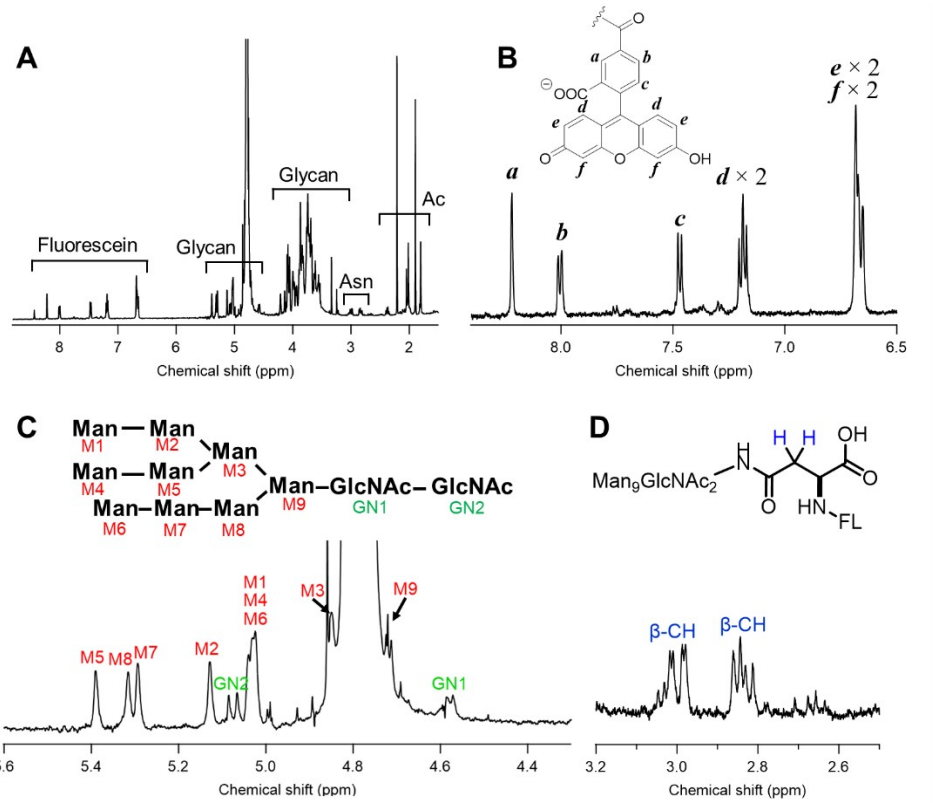

Fig. S2. ^{1}H NMR spectra of **M9-Asn-FL**: (A) overall and (B) enlarged spectra of the fluorescein moiety, (C) the anomeric proton signals of glycan moiety and (D) the Asn residue.

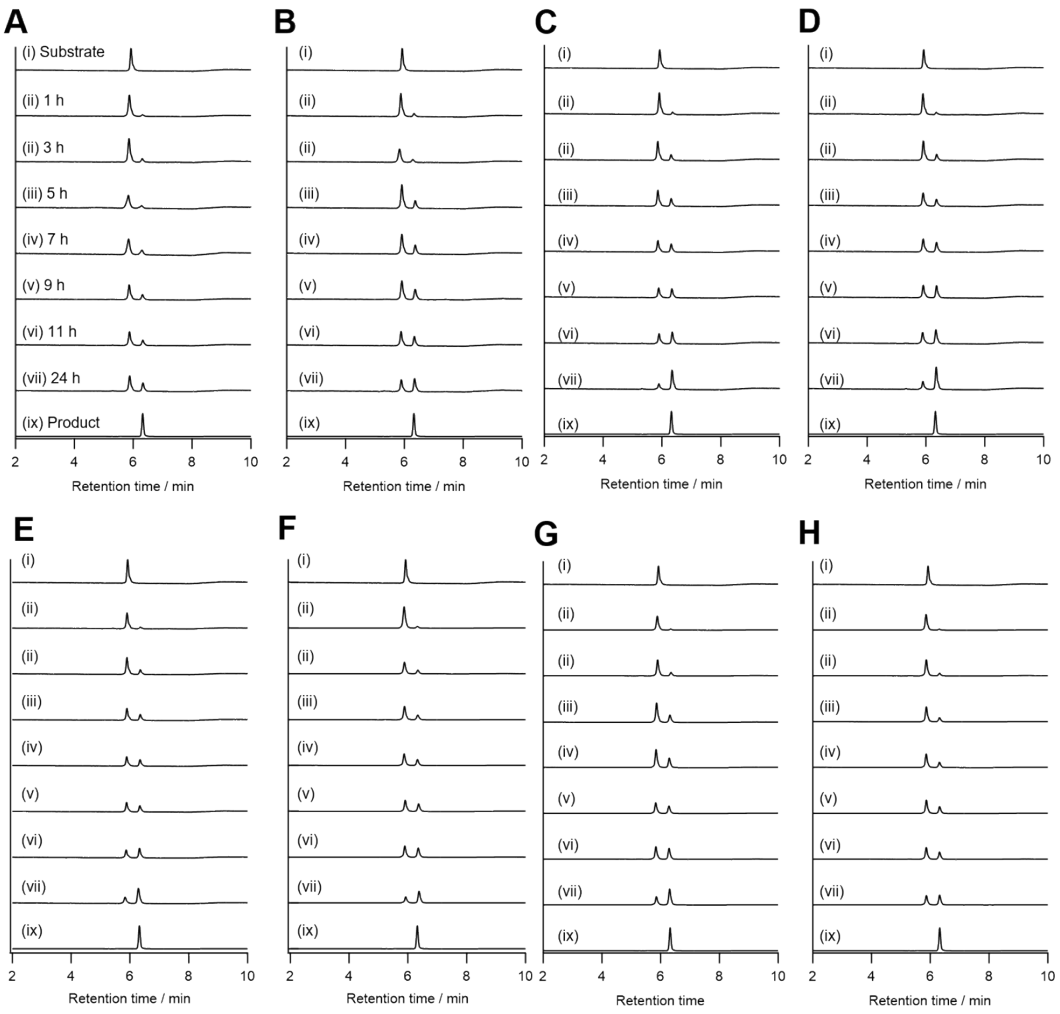

Fig. S3. UPLC elution profiles of UGGT1 enzymatic reaction with **M9-Asn-Fmoc**. Traces are shown, from top to bottom, for (i) authentic substrate **M9-Asn-Fmoc**, reaction mixture after (ii) 1 h, (iii) 3 h, (iv) 5 h, (v) 7 h, (vi) 9 h, (vii) 11 h, and (viii) 24 h, and (ix) authentic **G1M9-Asn-Fmoc**. Enzymatic reactions were performed in 10 mM MES buffer at (A) pH 5.5, (B) pH 6.0, and (C) pH 6.5; in 10 mM HEPES buffer at (D) pH 7.0, (E) pH 7.5 and (F) pH 8.0; and in 10 mM Bicine buffer at (G) pH 8.5 and (H) pH 9.0.

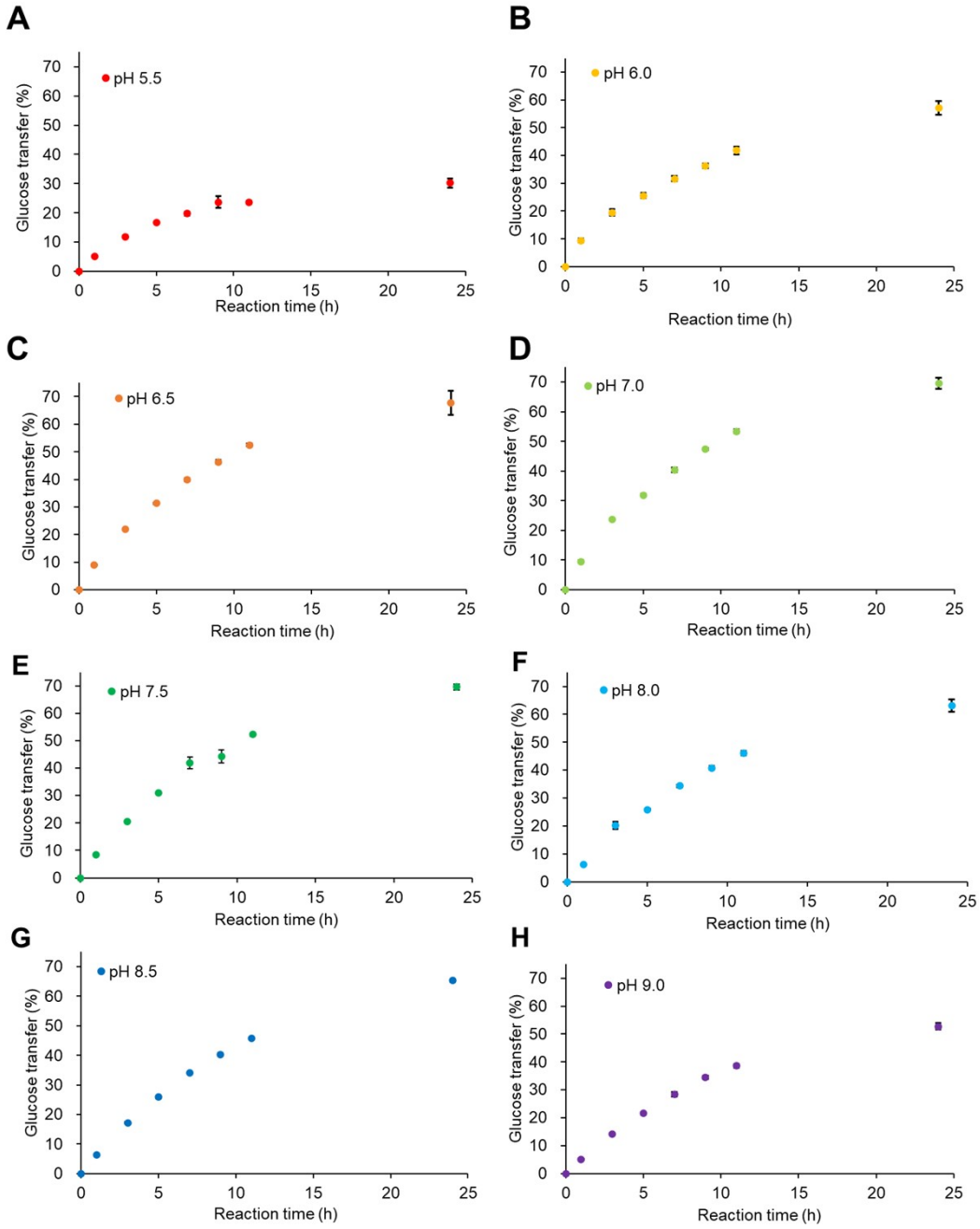

Fig. S4. UGGT1 glucose transfer activity toward **M9-Asn-Fmoc** measured in 10 mM MES buffer at (A) pH 5.5, (B) pH 6.0, and (C) pH 6.5; in 10 mM HEPES buffer at (D) pH 7.0, (E) pH 7.5 and (F) pH 8.0; and in 10 mM Bicine buffer at (G) pH 8.5 and (H) pH 9.0. The glucose transfer was determined from band area in UPLC: [**G1M9-Asn-Fmoc**] / ([**M9-Asn-Fmoc**] + [**G1M9-Asn-Fmoc**]). The data were average values from three independent experiments.

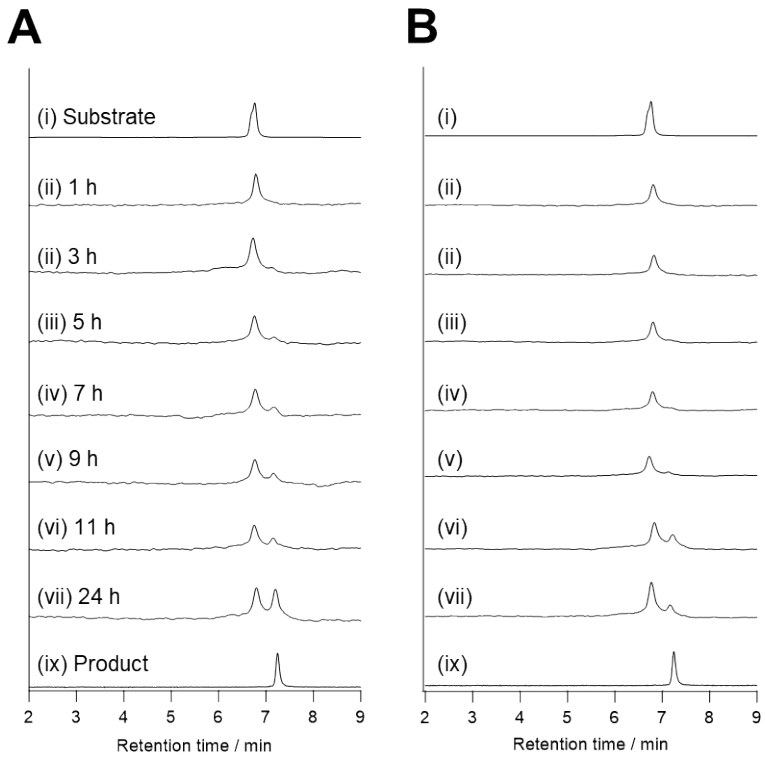

Fig. S5. UPLC elution profiles of UGGT1 enzymatic reaction with **M9-Asn-FL**. Traces are shown, from top to bottom, for (i) authentic substrate **M9-Asn-FL**, reaction mixture after (ii) 1 h, (iii) 3 h, (iv) 5 h, (v) 7 h, (vi) 9 h, (vii) 11 h, and (vi) 24 h, and (ix) authentic **G1M9-Asn-FL**. Enzymatic reactions were performed in 10 mM MES buffer at (A) pH 6.0; and in 10 mM Bicine buffer at (B) pH 8.5.

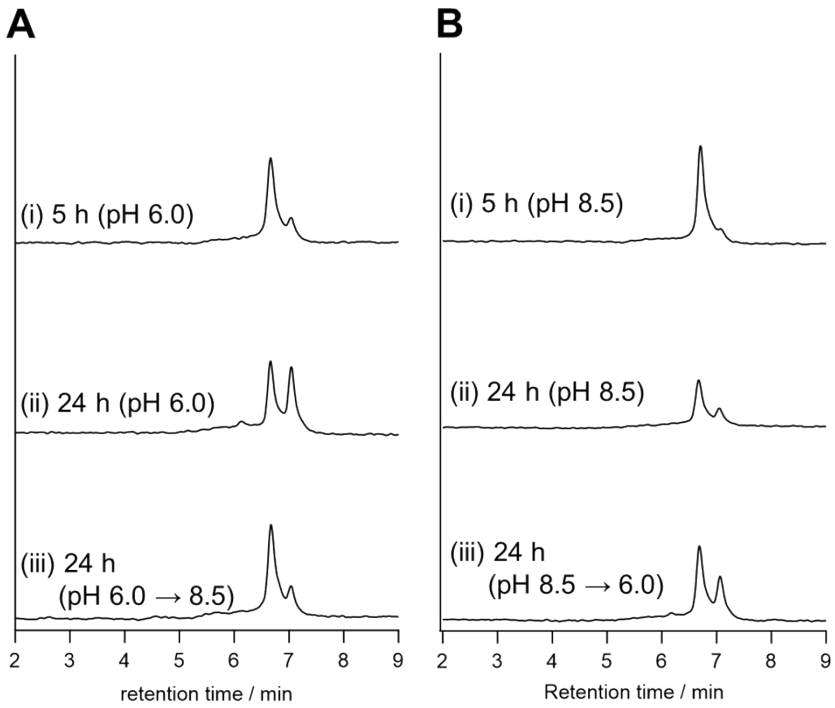

Fig. S6. UPLC elution profiles of UGGT1 enzymatic reaction with **M9-Asn-FL**. Traces are shown, from top to bottom, for reaction mixture after (i) 5 h and (ii) 24 h under maintaining pH condition, and (iii) 24 h under pH-shift condition (pH 6.0 to 8.5 and pH 8.5 to 6.0 at 5 h). Enzymatic assays were performed under constant pH conditions at (A) pH 6.0 (MES buffer) and (B) pH 8.5 (Bicine buffer).

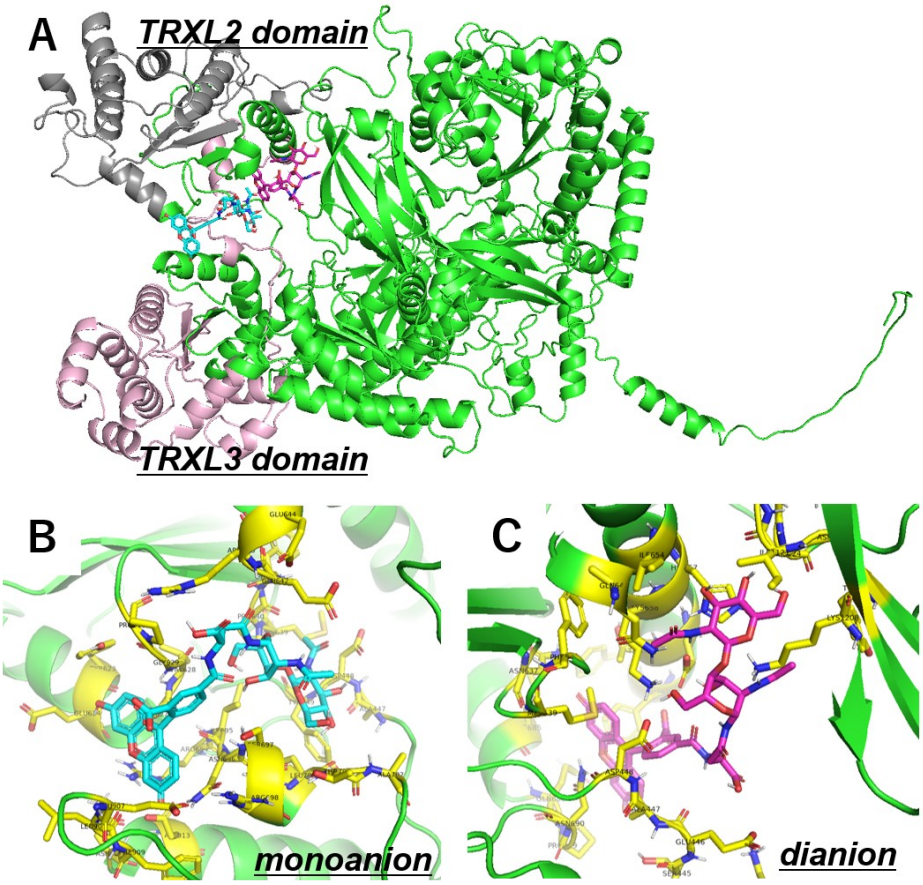

Fig. S7. Tentative docking models of **GlcNAc$_2$-Asn-FL** with the AlphaFold-predicted structure of human UGGT1. (A) Overall view of the docking models with the UGGT1 structure shown in green. Enlarged views of (B) the monoanionic form and (C) the dianionic form are shown. Carbon atoms of the monoanionic and dianionic ligands are colored cyan and magenta, respectively. Docking simulations were performed using a simplified glycan probe model and the AlphaFold-predicted structure of human UGGT1. The TRXL2 and TRXL3 domains are highlighted in gray and light pink, respectively. Amino acid residues located within 5 Å of the ligand are shown as carbon atoms colored yellow. Hydrogen, oxygen, nitrogen, and sulfur atoms are colored white, red, blue, and pale-yellow, respectively. The docking models suggest that the fluorescein aglycone may be accommodated near hydrophobic surface regions within the folding-sensor domain, including areas surrounding the TRXL domains that have been proposed to participate in substrate recognition. Because no experimentally determined UGGT1–substrate complex structure is currently available, these models should be regarded as hypothetical, hypothesis-generating models rather than direct evidence of the binding mode.

References

S1. (a) Y. Makimura, T. Kiuchi, M. Izumi, S. Dedola, Y. Ito, Y. Kajihara, *Carbohydr. Res*. **2012**, *364*, 41–48; (b) M. Hirose, Y. Nakamachi, H. Muto, A. Taira, S. Tanaka, T. Kuribara, K. Totani, *Carbohydr. Res*. **2024**, *540*, 109138.

S2. E. S. Trombetta, A. J. Parodi, *Methods* **2005**, *35*, 328–337.

S3. (a) C. Lee, W. Yang, R. G. Parr, *Phys. Rev. B* **1988**, *37*, 785–789; (b) A. D. Becke, *J. Chem. Phys*. **1993**, *98*, 5648–5652.

S4. (a) R. Ditchfield, W. J. Hehre, J. A. Pople, *J. Chem. Phys*. **1971**, *54*, 724–728; (b) W. J. Hehre, R. Ditchfield, J. A. Pople, *J. Chem. Phys*. **1972**, *56*, 2257–2261; (c) V. A. Rassolov, J. A. Pople, M. A. Ratner, T. L. Windus, *J. Chem. Phys*. **1998**, *109*, 1223–1229; (d) T. Clark, J. Chandrasekhar, G. W. Spitznagel, P. v. R. Schleyer, *J. Comput. Chem*. **1983**, *4*, 294–301.

S5. Gaussian 16, Revision C.01, M. J. Frisch, G. W. Trucks, H. B. Schlegel, G. E. Scuseria, M. A. Robb, J. R. Cheeseman, G. Scalmani, V. Barone, G. A. Petersson, H. Nakatsuji, X. Li, M. Caricato, A. V. Marenich, J. Bloino, B. G. Janesko, R. Gomperts, B. Mennucci, H. P. Hratchian, J. V. Ortiz, A. F. Izmaylov, J. L. Sonnenberg, D. Williams-Young, F. Ding, F. Lipparini, F. Egidi, J. Goings, B. Peng, A. Petrone, T. Henderson, D. Ranasinghe, V. G. Zakrzewski, J. Gao, N. Rega, G. Zheng, W. Liang, M. Hada, M. Ehara, K. Toyota, R. Fukuda, J. Hasegawa, M. Ishida, T. Nakajima, Y. Honda, O. Kitao, H. Nakai, T. Vreven, K. Throssell, J. A. Montgomery, Jr., J. E. Peralta, F. Ogliaro, M. J. Bearpark, J. J. Heyd, E. N. Brothers, K. N. Kudin, V. N. Staroverov, T. A. Keith, R. Kobayashi, J. Normand, K. Raghavachari, A. P. Rendell, J. C. Burant, S. S. Iyengar, J. Tomasi, M. Cossi, J. M. Millam, M. Klene, C. Adamo, R. Cammi, J. W. Ochterski, R. L. Martin, K. Morokuma, O. Farkas, J. B. Foresman, D. J. Fox, Gaussian, Inc., Wallingford CT, 2019.

S6. (a) J. Jumper, R. Evans, A. Pritzel, T. Green, M. Figurnov, O. Ronneberger, K. Tunyasuvunakool, R. Bates, A. Žídek, A. Potapenko, A. Bridgland, C. Meyer, S. A. A. Kohl, A. J. Ballard, A. Cowie, B. Romera-Paredes, S. Nikolov, R. Jain, J. Adler, T. Back, S. Petersen, D. Reiman, E. Clancy, M. Zielinski, M. Steinegger, M. Pacholska, T. Berghammer, S. Bodenstein, D. Silver, O. Vinyals, A. W. Senior, K.

Kavukcuoglu, P. Kohli and D. Hassabis, *Nature* **2021**, *596*, 583–589; (b) M. Mirdita, K. Schütze, Y. Moriwaki, L. Heo, S. Ovchinnikov, M. Steinegger, *Nat. Method* **2022**, *19*, 679–682.

S7. O. Trott, A. J. Olson, *J. Comput. Chem*. **2010**, *31*, 455–461.